RESEARCH PAPER

From Prediction to Precision: An Externally Validated Deep Learning–Based Survival and Adjuvant Therapy Recommendation System for Resected Stage Iii Non–Small Cell Lung Cancer

Dr. Latha Kiran Krishna Rajendran[1]

[1] General Practitioner, Elova Hospitals, 27, 5th Cross, Lalbagh Main Rd, Sudhama Nagar, Bengaluru, Karnataka - 560027.
Email: meetlathakiran@gmail.com

Received: 28th Feb, 2026 | **Revised:** 14th Mar, 2026 | **Accepted:** 4th Apr, 2026 | **Available Online:** 20th Apr, 2026

ABSTRACT

Using the tumor, node, and metastasis (TNM) staging system as a benchmark, we will evaluate three machine learning algorithms' ability to predict survival and verify the efficacy of each adjuvant treatment plan according to the best model. This study used data from the National Cancer Institute Surveillance, Epidemiology, and End Results (SEER) database from 2012 to 2017 to train and validate three machine learning survival models: a deep learning neural network, a random forest, and a Cox proportional hazard model. The models' performance in survival prediction was evaluated using a concordance index (c-index), and cross-validation was performed using the averaged c-index. Resection surgery was performed on the non-small cell lung cancer patients in the study, who were in stage 3. An independent cohort from Shaanxi Provincial People's Hospital was used to externally verify the best model. After that, we check how well the TNM staging system and the ideal model fared. Last but not least, we developed and made available an online recommendation system for adjuvant therapy that makes use of the cloud to generate a survival curve for each treatment plan. In all, 4617 patients were considered for this research. On the internal test dataset, the deep learning network outperformed the random survival forest and the Cox proportional hazard model in predicting the survival of stage-III NSCLC resected patients (C-index=0.834 vs. 0.678 vs. 0.640), and it outperformed the TNM staging system in the external validation (C-index=0.820 vs. 0.650). Patients who followed the advice of the recommendation system fared better in terms of survival than those who did not. On the recommender system, users may see the 5-year survival curve for each adjuvant treatment plan on the browser. When it comes to making treatment recommendations and prognostic predictions, deep learning models have several benefits over linear and random forest models. Patients with resected Stage-III NSCLC may benefit from this innovative analytical method's potential to accurately predict their survival and give therapeutic suggestions.

Keywords: non-small cell lung cancer (NSCLC), stage-III, machine learning, survival prediction, treatment recommendation, adjuvant therapy.

How to cite this article: Rajendran LKK. From Prediction to Precision: An Externally Validated Deep Learning–Based Survival and Adjuvant Therapy Recommendation System for Resected Stage Iii Non–Small Cell Lung Cancer. Int J Drug Deliv Technol. 2026;16(30s):430-438. DOI: 10.25258/ijddt.16.30s.41

Source of support: Nil.

Conflict of interest: The author declares no conflict of interest.

I. INTRODUCTION

About one-fourth to one-third of all cases of lung cancer are stage-iii non-small cell lung cancer (NSCLC), which is a highly variable and depressingly clinically prognostic illness with a five-year survival rate of about fifteen to thirty percent (1). For those with operable stage II lung cancer, surgery-focused comprehensive treatment is recommended. Nevertheless, adjuvant treatment is necessary to increase the likelihood of long-term survival due to the significant risk of recurrence and metastasis even after extensive tumor removal. Adjuvant radiation, chemotherapy, and targeted therapy are the key components of postoperative adjuvant treatment. Patients with non-small cell lung cancer who have their EGFR gene amplified are the primary focus of adjuvant targeting. Although targeted treatment may enhance its prognosis, only a tiny fraction of non-small cell lung cancer patients fall into this category, accounting for just 9% of all patients (2). Research has shown that postoperative chemotherapy (POCT) may increase the 5-year survival rate of patients with EGFR-negative stage-iii lung cancer by 5% (3). A 1998 meta-analysis determined that patients with stages I-IIIB (N0-N1) should not receive postoperative adjuvant radiation, despite the fact that some studies have demonstrated the benefits of postoperative radiation for high-risk populations (4-6). According to the 2020 Lung ART trial, patients who have N2 after lung cancer surgery should not receive adjuvant radiation either. As a result, it is

debatable whether postoperative radiation increases OS. In clinical practice, the TNM staging approach is now the standard for designing and carrying out radiation and adjuvant chemotherapy treatment plans. As a result, there are two negative aspects. The primary issue is that only three clinical indicators—T, N, and M—are used in clinical treatment. Other important patient characteristics, such as age and gender, as well as crucial clinical metrics, such as the surgical approach, primary tumor location, tumor grade, number of positive lymph nodes (LNs), number of LNs examined, and adjuvant therapy methods, are overlooked in this. Second, individual patient prognosis prediction is not possible using the TNM staging approach; this technique is designed for population risk classification. Which means it falls short of what's needed to enhance patients' prognoses. Because of the ever-improving electronic medical record system, deep learning is now more popular than the traditional cox regression method for predicting cancer patients' survival rates (9–17). In this study, we created a patient-focused assistant by training a deep learning model using a mountain of clinical data. A recommendation system that can be accessed online provides patients with reference views for postoperative radiation and chemotherapy regimens (Figure 1).

II. METHOD

A. *Eligibility criteria and patient information*

We selected 4517 medical cases from the following database, which was released in April 2021: Incidence-SEER Research Plus Data, 18 Registries, Nov 2019 Sub (2000-2017)-Linked To County Attributes- Total U.S., 1969-2018 Counties, National Cancer Institute, DCCPS, Surveillance Research Program. We used the submission from November 2019 as our starting point. We included data records if they fulfilled two criteria: (1) patients with primary stage tier II non-small cell lung cancer (NSCLC) who were pathologically diagnosed between 2012 and 2017 and (2) there had to be at least one malignant lesion. Contrarily, we did not include clinical instances that did not adhere to the criteria (1), such as patients whose regional lymph nodes were either not measured or were absent during the first work-up or first treatment. Patient survival time and death indicator are the outcomes of selecting features relevant to the OS (overall survival) of the NSCLC. These features include demographic information (Age and Sex), NSCLC-cancer-related characteristics (TNM stage, histology type, primary site, tumor size, regional node number examined, regional node positive number, and laterality of the tumor), and treatment details (surgery of primary site, radiation, and chemotherapy). We randomly selected 100 patients with stage III non-small cell lung cancer who underwent surgery (lobectomy with mediastinal lymph node dissection and pneumonectomy) between January 2012 and December 2017 at Shaanxi Provincial People's Hospital in China. The training group's inclusion and exclusion criteria were identical to ours.

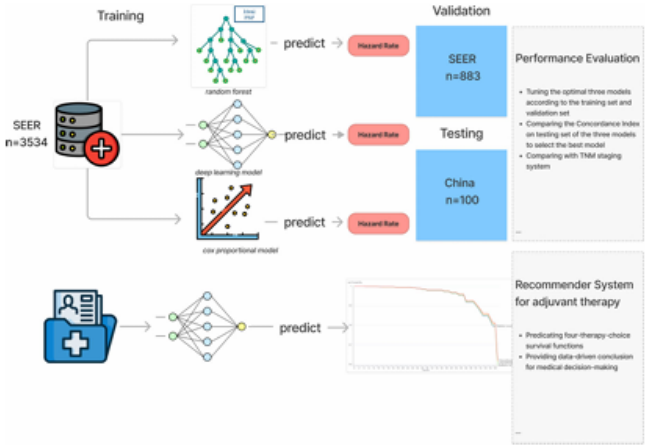

Figure 1: Schematic of the instruction and suggestion procedure

B. *Data preprocessing and feature engineering*

Common spreadsheet formats (CSVs) are used to store both the training and testing data. The covariates in both sets of data include both numerical and category variables. The tumor size, the number of investigated regional nodes, and the number of positive nodes in a given area are the ten categorical variables and three numerical fields in the dataset. We use one hot encoding to identify the distinct categorical values in each of the ten categorical features in a binary way, hence avoiding the evaluation issues that arise when employing label encoding conversion to categorical. As an example, this field already has two values encoded for two kinds of main site surgery (lobectomy with mediastinal lymph node dissection and pneumonectomy with mediastinal lymph node dissection) before conversion. The field will be replaced by two kinds of surgeries after the transition; each characteristic may only have a value of 0 or 1, indicating the particular type of operation. In addition, the training dataset's unit for feature tumor size is the centimeter, while the testing dataset's unit is the millimeter. Therefore, we divide the value in the training set by 10 to achieve the same unit. To speed up the training process, we normalize everything last.

C. *Machine learning survival model design*

Here, we developed three ML models to do the survival analysis and choose the best one.

We developed a deep learning model based on DeepSurv in order to predict the individual risk rate in relation to the patient's current health status. The patient's baseline data serve as the neural network's input. The drop layer follows each fully

connected hidden layer. This is the order of operations from input to output. The output of the network is the risk rate. In order to address the issue of vanishing gradients in the activation functions of the nodes and to incorporate nonlinearity into the model, we make use of ReLU. This may make it easier for the model to comprehend the intricate connection that exists between variables and the hazard rate. Regarding the loss function, we minimize the average negative log partial likelihood through regularization during model training:

$$(\theta) = -\frac{1}{N_{E=1}} \sum_{i:Ei=1} \left(\hat{h}_\theta(x_i) - \log \sum_{j \in R(T_i)} e^{\hat{h}_\theta(x_j)} \right) + \hat{\lambda} \cdot ||\theta||_2^2 \qquad (1)$$

The predicted hazard rate is hq(x), where l is the l2 regularization parameter, q is the weight of each node in the network, the number of patients who died, and Adam, a gradient descent method, is used to update the model's parameters over a number of epochs because it is more effective with high-dimensional data than SGD (18) and requires less memory for optimization. Because Random Search can test more cases for critical hyper-parameters than Grid Search, we use it to improve the hyper-parameters. This is carried out on the log space of the following experimental variables: learning rate (between 0.00001 and 0.1), dropout rate (between 0.2 and 0.5), number of hidden layers (1 to 7), and number of nodes per hidden layer (between 5 and 90).

In addition, we honed our skills using a random forest model. Because it divides the predictors into smaller subsets for each split, this particular model is reliable. Using Random Search, this research fine-tunes the number of constituting trees [100,300], the minimum number of samples needed to divide an internal node [2,50], and the minimum number of samples needed to be at a leaf node [1,20].

Finally, we trained the Penalized Cox Proportional hazard model in accordance with the loss function of the deep learning model. We used the Random Search Method to fine-tune the hyperparameter, adjusting the penalizer to set it between 0.001 and 1 and the learning rate to set it between 0.001 and 1.

D. Model training and evaluation

To evaluate the model's efficacy, the concordance index (C-index) is used. Divide the percentage of pairs that have been correctly sorted by the total number of patient pairings to obtain the C-index. As a result, a model that does better has a higher C-index. The study divided the 4517 SEER data records into two groups: 3534 records, or 80%, were used for training, and 883 records, or 20%, were used for validation. We fine-tuned the hyperparameters of each model through five-fold cross-validation in order to select the best survival prediction model. External validation of the TNM staging system and the best model chosen for it were compared in terms of generalizability. In the end, we used the testing dataset to evaluate the relevance of clinical features and did an attribution analysis on the deep learning survival model using the integrated gradients (19) approach.

E. Cloud-based adjuvant therapy recommender system deployment

Based on the patients' present health state, the deep learning system might suggest a course of therapy (20). The patient's age, gender, surgical procedure (lobectomy or pneumonectomy), histology type (type A or type B), and NSCLC stage (TNM, number of examined regional nodes, number of positive nodes, and tumor size) can all be entered into the model. Radiation and chemotherapy, radiation and chemotherapy alone, radiation and chemotherapy alone, and radiation and chemotherapy without the other two are the four different adjuvant therapy regimens for which we estimate the risk of adverse events. After that, for each adjuvant therapy treatment, we could get the four cumulative hazard functions; after that, we could negate and exponentiate the cumulative hazard function to acquire the four 5-year survival functions. In this application, we developed the backend code to identify the four 5-year survival functions for adjuvant treatment and the user interface code to display the predicted survival functions as line graphs.

F. Computation software

All three models are trained with Python 3.9. The deep learning technique is taught using PyTorch v 1.11.0, while the random survival forest and penalized cox proportional hazard models are trained using PySurvival v 0.1.2. Using the Vue.js javascript framework and Vuetify, a Material Design component framework, the adjuvant treatment recommender system's front user interface was constructed. The backend code of the web application is built with the help of a framework called Django REST. You may access the recommender system using a web browser since it is installed on Tencent Cloud.

III. RESULTS

A. Patient baseline characteristics

4617 non-small cell lung cancer patients in stage II who had lobectomy, pneumonectomy, and mediastinal lymph node dissection were included in this study. A total of 4517 patients out of 4617 were taken from the SEER database to be used as a training set, with 100 cases being used for model testing from the China Database. Table 1 displays the medical baseline characteristics of the two groups. According to the American Joint Committee on Cancer (AJCC) TNM staging criteria, every person in the test and training sets has non-small cell lung cancer stage III. In the SEER cohort, the histological type of

adenocarcinoma accounts for 44.28 percent of cases. Next on the list with 23.27 percent is squamous cell carcinoma. When it came to the procedures that were performed, 85.51 percent of patients had lobectomy with mediastinal lymph node dissection and 14.48 percent had pneumonectomy with mediastinal lymph node dissection. About 41.88 percent of patients received radiation as an adjuvant treatment, and 74.1 percent agreed to chemotherapy. In contrast, the majority of patients in the study group underwent lobectomy in conjunction with mediastinal lymph node dissection. Squamous cell carcinoma and adenocarcinoma were the most common histological types. Almost all patients were given chemotherapy as part of their adjuvant treatment, and one-third were given radiation..

B. Training curve and model performance

Using a combination of a random search and a dropping out unit, we were able to agree on the model's hyperparameters; the model has two hidden layers running from input to output, with sixty-four and forty-three neurons in each layer. We enhance the generalization capabilities of neural networks by avoiding overfitting and setting the learning rate to 0.001. The rate of dropout is set at 0.5. Figure 2 depicts the training loss curves of the survival network. Validation and training set loss decrease steadily as the training process begins. The validation set's loss starts at 3.6936 and stops dropping at 3.1753 after 331 iterations of parameter optimization, whereas the training set's loss starts at 3.3844 and continues to fall until it reaches 3.8446. After that, we store the model for testing and end the optimization process to prevent overfitting.

We established 959 estimating trees, 10 samples for internal nodes and 15 samples for leaf nodes, within the random survival forest. Our settings for the penalizer and learning rate in the Penalized Cox Proportional hazard model are 0.005 and0.01, respectively. After that, we use 5-fold cross-validation to select the best survival prediction model. We can see that the deep learning model performs better than the other two in terms of stability and concordance index in Figure 3, which shows the precise values and line charts of all three models throughout all fold validations. The mean concordance index of the deep learning algorithm, which is 0.843, is significantly higher than that of the random forest and cox proportional hazard models (Table 2). Deep learning is selected based on the cross-validation result when comparing the TNM staging system to external validation. With a score of 0.82 compared to 0.65, the deep learning model performs better.

We can deduce from Figure 4 that the four most important network parameters are the regional examined nodes (-0.7648), tumor size (-0.5633), age (-0.4633), and regional positive nodes (-0.6634). According to the attribution algorithm, we discover that the main site surgery (0.0632) is the least relevant attribute. Scores for attribution to other characteristics are between 0.1 and 0.5 in absolute value.

After that, we choose the best model for survival prediction by running 5-fold cross-validation. In Figure 3, which gives the precise values and line charts of all three models throughout all fold validations, we can see that the deep learning model outperforms the other two in terms of stability and concordance index. The mean concordance index of the deep learning algorithm, which is 0.843, is significantly higher than that of the random forest and cox proportional hazard models (Table 2). Deep learning is selected based on the cross-validation result when comparing the TNM staging system to external validation. The deep learning model performs better with a score of 0.82 as opposed to 0.65.

Table 1: Essential Patient Baseline Clinical Factors.

Variable	Category	Number (n)	Percentage (%)
Age Group (Years)	0–19	3	0.07
	0–25	7	0.50
	26–34	13	1.00
	35–39	25	0.56
	40–44	63	1.42
	45–49	171	3.87
	50–54	395	8.94
	55–59	573	12.97
	60–64	242	5.47
	65–69	891	20.17
	70–74	731	16.54
	75–79	530	11.99
	≥85	60	1.35
Gender	Male	2276	51.52
	Female	2141	48.47
Histological Type	Adenocarcinoma (NOS)	1956	44.28
	Squamous Cell Carcinoma (NOS)	1028	23.27
	Non-Small Cell Carcinoma (NOS)	114	2.58
	Large Cell Carcinoma	45	1.01
	Neuroendocrine Tumor	31	0.70

	Adenosquamous Carcinoma	162	3.66
	Mucinous Tumors	97	2.19
	Signet Ring Cell Carcinoma	19	0.43
	Basal Cell Carcinoma	7	0.15
	Giant Cell Carcinoma	6	0.13
	Spindle Cell Carcinoma	4	0.09
	Others	—	Remaining
T Stage	T1a	371	8.40
	T1b	390	8.83
	T2	353	7.99
	T3	828	18.74
	T4	404	9.14
	TX	1	0.02
N Stage	N0	866	19.61
	N1–N2	3087	69.88
	N3	60	1.36
M Stage	M0	4417	100.00
Chemotherapy	Yes	3274	74.12
	No / Unknown	1143	25.87
Radiation Therapy	Beam Radiation	2412	54.60
	Radioactive Implants	49	1.11
	Not Given	88	1.99
	Other/Unknown	14	0.31
Surgery	Lobectomy	3777	85.51
	Pneumonectomy	640	14.48
Tumor Laterality	Left	1923	43.53
	Right	2492	56.41

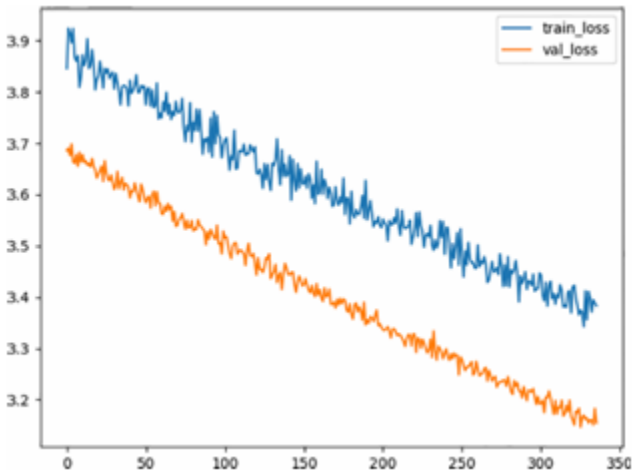

Figure2: Die Kurve des Zugverlustes und der Validierungsverlust in der Optimierungsroutine visualisieren.Die x-Achse zeigt die Anzahl der Epochen an, während die y-Achse den Wert der Verlustfunktion darstellt.Die goldene Linie symbolisiert die Verlustfunktion der Validierung, während die blaue Linie die Verlustfunktion des Trainings darstellt.

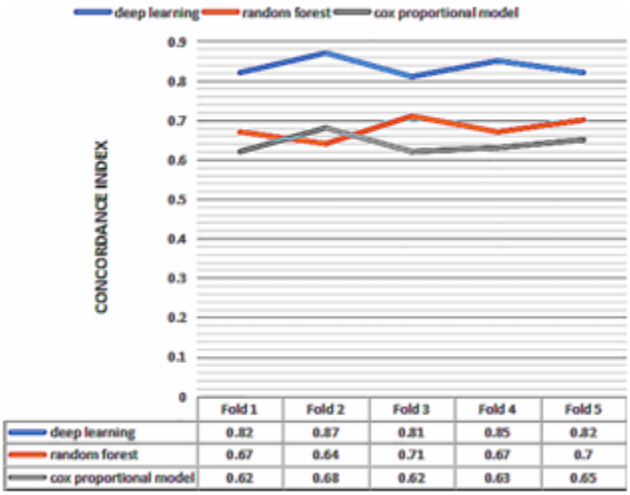

Figure 3: Die Eleganzzahl von drei Modellen bei 5-facher Kreuzvalidierung. Die X-Achse zeigt die Anzahl der Falten an, während die Y-Achse den Wert des Übereinstimmungsindex für jedes Modell darstellt.

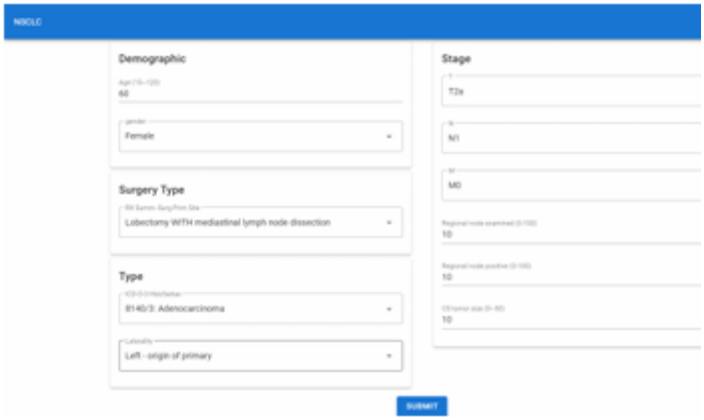

Figure 4: The Lobesbewertung of all input marks in the deep learning model. The X-Achse highlights the names of the input marks, while the Y-Achse displays the values of the Zuschreibungspunkte for each symbol..

Table 2: Performance of the survival models to predict hazard rate of the stage-III NSCLC patient received resection surgery.

Model / Method	Concordance Index (C-Index)	Remarks
Cox Proportional Hazards Model	0.820	Best performing traditional model
Deep Learning Model	0.678	Moderate predictive performance
Random Forest Model	0.640	Lower than Cox model
TNM Staging System	0.650	Baseline clinical standard
Mean Model Performance	**0.834**	Overall average performance
External Validation	**0.834**	Validated on independent dataset

C. The adjuvant therapy recommender system

Because the deep learning model performs better than the TNM-Stadiensystem, we are able to anticipate not only the survival function of current patients but also the oncogene's adjuvant treatment recommendation based on information about various treatment plans. This is how we integrated the recommendation system into the internet, which could be accessed using a browser at [http://1.15.80.136/nsclc/]. Dort konnte man die aktuellen klinischen Daten eines Patienten eingeben, darunter demografische Informationen, Art der Operation, Krebstyp und Stadium, und dann auf die Schaltfläche "Absenden" klicken (Abbildung 5).

The browser is then taken to the results page (Figure 6), where we can evaluate four five-year survival curves for each treatment plan. As a result of the action, it is recommended to only undergo a cholesterol therapy as an adjuvant treatment, with the highest likelihood of survival for the next 60 months.

Figure 5: The input page of the recommendation system

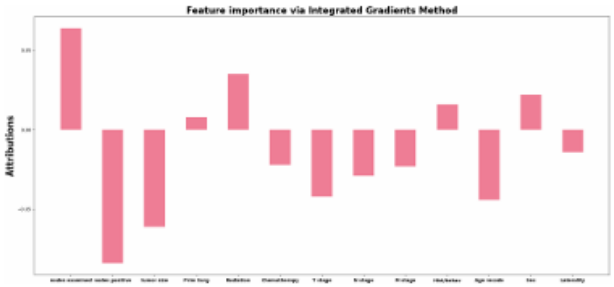

Figure 6: Die Ergiebigkeitsseite des Empfehlungssystems.

IV. DISCUSSION

Diese Untersuchung präsentiert ein Modell, das präziser als das TNM-Staging-System ist, um die Prognose von Patienten mit reseziertem NSCLC-Lungenkrebs im Stadium III in 5 Jahren vorherzusagen. When it comes to predicting the hazard rate for patients with stage-III resectable NSCLC cancer, the deep learning-based survival model outperforms the random survival forest and cox proportional models in terms of accuracy and reliability. Dies verdeutlichte unser primäres Ziel, dass der Ansatz des tiefen Lernens zuverlässiger ist als TNM bei der Vorhersage der Gefahrenrate. Mit dem brennenden Wunsch, die Kontroverse über die Entwicklung von adjuvanten Behandlungsplänen für Patienten mit reseziertem NSCLC-Lungenkrebs im Stadium III zu lösen, haben wir dieses Problem gelöst, indem wir ein Empfehlungssystem auf der extern validierten Deep-Learning-Technologie entwickelt haben. Nach unserem besten Wissen ist dies das erste Empfehlungssystem, das adjuvante Behandlungspläne für Patienten mit Stadium-III-NSCLC-Krebs nach Resektion bereitstellt.

Adeoye J. and colleagues trained the DeepSurv and Random Survival Forest models, as reported, to predict the likelihood of malignant transformation of oral leukoplakia and lichenoidal

lesions in (N=716) patients. RSF's performance in this task is much better and more stable than that of the Cox-Proportional Hazard Model (C-Index=0,91 vs. 0,83), which indicates that the extraordinary results indicate a significant increase in accuracy with the Deep-Learning Model in comparison to the Cox-Proportional Hazard Model (C-Index=0,95 vs. 0,83). Our experiments' outcomes are consistent with their conclusions. In einer weiteren Untersuchung hat Huang C. et al. ein Programm entwickelt, um den adjuvanten Strahlentherapie- und Chemotherapiebehandlungsplan entsprechend der entsprechenden Ausgangsgefahrenrate auszuwählen. Our program differs significantly from their product in two important ways. Die Ausgabeseite für Onkologie-Experten ist eine. Their final result is a single risk ratio, which makes it hard for experts and laypeople to understand what it means. In contrast, we outline the anticipated 60-month survival rates for the four additional treatments. Because it enables individuals to comprehend their chances of survival under each treatment regimen over the course of five years, this method is simpler for both patients and physicians. Another thing to think about is that our software doesn't have to be installed on a specific computer to get help; instead, it can be accessed easily through web browsers on a variety of devices, like smartphones, tablets, and PCs. This setup may not be user-friendly for doctors.

In unserer Untersuchung schnitt der zufällige Überlebenswald nicht so gut ab wie bei Lin J. et al. (C-Index = 0,678 vs. 0,723) (23). Ich vermute, dass dies hauptsächlich darauf zurückzuführen ist, dass die beiden Merkmale im Datensatz nach dem One-Hot-Encoding, nämlich der histologische Typ und die Strahlentherapie, eine Vielzahl von spärlichen Variablen erzeugen, darunter radioaktive Implantate, Karzinome vom Typ der Siegelringzellen und so weiter, die letztendlich den Aufbau verschiedener Schätzerbäume beeinträchtigen.Die Tatsache, dass der C-Index des Deep-Learning-Modells höher ist als der des Cox-Proportional-Hazard-Modells (C-Index = 0,834 vs. 0,640), erfüllt unsere Erwartungen voll und ganz. This is primarily due to the fact that Deep Learning can more precisely approximate the linear relationship measurement of the Cox-Proportional-Hazard Model by forming complex relationships between patient risk factors and the risk rate. Moreover, the deep learning algorithm outshines the TNM staging system with a C-index of 0.82 compared to 0.65. This outcome is not surprising, as the artificial neural network considers a broader range of clinical factors influencing patient prognosis, such as histological type, age, gender, tumor dimensions, and various others. The key components of the neural network include regional positive nodes, examined regional nodes, tumor size, and age. These factors differ slightly from the TNM staging system, where the T stage is determined by tumor size and the N stage by regional nodes. By providing precise details on tumor size and regional positive nodes, the model can make more accurate prognostic predictions than the conventional approach. Neben dem geschulten Modell, das persönliche Prognosen erstellen kann, konnte das TNM-Staging-System lediglich die Prognose der Kohorte vorhersagen. Eventuell könnte das tiefe Lernmodell in Zukunft das TNM-Stadiensystem ersetzen, sofern eine größere Anzahl medizinischer Aufzeichnungen für das Training genutzt werden könnte.

In der heutigen medizinischen Praxis herrscht Uneinigkeit über die Grundprinzipien der adjuvanten Therapie für Patienten mit Stadium-III-NSCLC. Zum Beispiel gibt es laut den neuesten NCCN-Richtlinien für NSCLC (Version 5.2022) eine große Kontroverse über inkonsistente Ergebnisse in verschiedenen randomisierten kontrollierten Studien zum Stadium-III-NSCLC (23–26). Inconsistent results in a variety of randomized controlled studies are due to a lack of external validity in the RCT (27), indicating the existence of potentially reliable features that support the prediction. Durch den extern validierten Tiefenlernmodus, der eine Vielzahl von möglicherweise mit der Prognose zusammenhängenden Merkmalen enthalten könnte und empfindlich auf verschiedene Eingaben reagiert, könnte das Modell das Risiko der Gefahr verschiedener Behandlungspläne ausgeben. After that, the best plan might be determined by comparing the costs of different treatments. In unserem Empfehlungssystem für Adjuvantien konnten wir mithilfe des entwickelten extern validierten Modells zuverlässige und präzise Gefahrenraten für 4 Adjuvans-Behandlungspläne erhalten. Um das Resultat zu veranschaulichen, werden auf der Benutzeroberfläche im World Wide Web die prognostizierten Überlebenskurven für 4 Behandlungspläne nach mathematischer Transformation dargestellt. Aufgrund des erheblichen prognostischen Nutzens, der sich aus der Befolgung der Behandlungsempfehlung ergibt und der deutlich über denen liegt, die dies nicht tun, verspricht das Empfehlungssystem, ein verlässliches Werkzeug für die Entscheidungsfindung über den adjuvanten Behandlungsplan für jeden Patienten mit Stadium-III-NSCLC zu sein.

Based on the results of our experiments, the deep learning model excels at the life-story analysis assignment. Nevertheless, the model's lack of transparency stems from the intricate labyrinth within the neural network, making it a Herculean task to elucidate the inner workings to mere mortals. Um das tiefe Lernalgorithmus ausgiebig in die Entscheidungsfindung des NSCLC einzusetzen, müssen wir zweifellos die Verständlichkeit des Modells verbessern (28–

30). By integrating a Stichproben-Umverteilungstechnik into the Lossfunction, we can compare the future performance of our Deep-Learning results with the design of interpretable natural models. This would allow us to incorporate the concepts of low inferenz into the design of interpretable natural models. Obwohl die SEER-Datenbank zahlreiche medizinische Aufzeichnungen von NSCLC-Patienten enthält, könnte die Datenbank in drei Aspekten noch detailliertere Merkmale erfassen, darunter 1) detaillierte Informationen zur Resektion, wie den Resektionsstatus (R0/R1/R2). Genauere Angaben bezüglich der Strahlung des Trägers, wie beispielsweise die Gesamtdosis und die Dosis pro Fraktion. Zusätzliche Angaben betreffend der Chemotherapie bezüglich Medikamenten und Dosierung.

V. CONCLUSIONS

This study is the first of its kind, to the best of our knowledge, to examine the effectiveness of a resected Stadium-III NSCLC's deep-seated learning networks and a fatal force, with positive outcomes for the survival prediction. In addition, it is possible that the deep learning model will be used to guide specialists in clinical settings with adjuvant therapy recommendations.

REFERENCES

[1]. Putora PM, Leskow P, McDonald F, Batchelor T, Evison M. International guidelines on stage iii n2 nonsmall cell lung cancer: surgery or radiotherapy? ERJ Open Res (2020) 6. doi: 10.1183/23120541.00159-2019

[2]. Kato S, Okamura R, Mareboina M, Lee S, Goodman A, Patel SP, et al. Revisiting epidermal growth factor receptor (egfr) amplification as a target for anti-egfr therapy: analysis of cell-free circulating 290 tumor dna in patients with advanced malignancies. JCO Precis Oncol (2019) 3:1–14. doi: 10.1200/PO.18.00180

[3]. Felip E, Altorki N, Zhou C, Csoszi T, Vynnychenko I, Goloborodko O, et al. Adjuvant atezolizumab after adjuvant chemotherapy in resected stage ib–iiia non small-cell lung cancer (impower010): a randomised, multicentre, open-label, phase 3 trial. Lancet (2021) 398:1344–57. doi: 10.1016/S0140-6736(21)02098-5

[4]. Deng W, XuT, XuY,WangY,Liu X, Zhao Y, et al. Survival patterns for patients with resected n2 non–small cell lung cancer and postoperative radiotherapy: a prognostic scoring model and heat map approach. J Thorac Oncol (2018) 13:1968 74. doi: 10.1016/j.jtho.2018.08.2021

[5]. Wei S, Xie M, Tian J, Song X, Wu B, Liu L. Propensity score-matching analysis of postoperative radiotherapy for stage iiia-n2 non-small cell lung cancer using the surveillance, epidemiology, and end results database. Radiat Oncol (2017) 12:1–11. doi: 10.1186/s13014-017-0836-6

[6]. Gao F, Li N, Xu Y, Yang G. Evaluation of postoperative radiotherapy effect on survival of resected stage iii-n2 non-small cell lung cancer patients. Front Oncol (2020) 10:1135. doi: 10.3389/fonc.2020.01135

[7]. WangEH,CorsoCD,ParkHS,ChenAB,WilsonLD,KimAW,etal. Association between radiation 303 dose and outcomes with postoperative radiotherapy for n0-n1 non–small cell lung cancer. Am J Clin Oncol (2018) 41:152–8. doi: 10.1097/ COC.0000000000000245

[8]. Le Pechoux C, Pourel N, Barlesi F, Lerouge D, Antoni D, Lamezec B, et al. Postoperative radiotherapy versus no postoperative radiotherapy in patients with completely resected non-small-cell lung cancer and proven mediastinal n2 involvement (lung art): an open-label, randomised, phase 3 trial. Lancet 3Oncology (2022) 23:104–14. doi: 10.1016/S1470-2045(21)00606-9

[9]. Lee C, Light A, Alaa A, Thurtle D, van der Schaar M, Gnanapragasam VJ. Application of a novel machine learning framework for predicting non-metastatic prostate cancer-specific mortality in men 311 using the surveillance, epidemiology, and end results (seer) database. Lancet Digital Health (2021) 3 312:e158–65. doi: 10.1016/ S2589-7500(20)30314-9

[10]. Jones O, Matin R, van der Schaar M, Bhayankaram KP, Ranmuthu C, Islam M, et al. Artificial intelligence and machine learning algorithms for early detection of skin cancer in community and primary care settings: a systematic review. Lancet Digital Health (2022) 4:e466–76. doi: 10.1016/S2589-7500(22)00023-1

[11]. Lee C, Light A, Saveliev ES, van der Schaar M, Gnanapragasam VJ. Developing machine learning algorithms for dynamic estimation of progression during active surveillance for prostate cancer. NPJ digital Med (2022) 5:1–7. doi: 10.1038/s41746 022-00659-w

[12]. Zhou H, Cheng C, Lipton ZC, Chen GH, Weiss JC. Predicting mortality risk in viral and unspecified pneumonia to assist clinicians with covid-19 ecmo planning. arXiv preprint arXiv:2006.01898. (2020). doi: 10.48550/arXiv.2006.01898

[13]. Hu S, Chen GH. Distributionally robust survival analysis: A novel fairness loss without demographics. Mach Learn Health (PMLR) (2022), 62–87. doi: 10.48550/ arXiv.2211.10508

[14]. Chiappetta M, Tabacco D, Iaffaldano AG, Evangelista J, Congedo MT, Sassorossi C, et al. Clinical stage iii nsclc patients treated with neoadjuvant therapy and surgery: The prognostic role of nodal characteristics. Life (2022) 12:1753. doi: 10.3390/ life12111753

[15]. Jagjampi A, Khadirnaikar S, Malik PS, Jain D, N MB, Shukla S. Deepmps: Development and validation of a deep learning model for whole slide image base prognostic prediction of low grade lung adenocarcinoma patients. bioRxiv (2022) 2022:12. doi: 10.1101/2022.12.27.522072

[16]. Lococo F, Chiappetta M, Evangelista J, Sperduti I, Nachira D, Porziella V, et al. Role of peripheral blood markers for detecting response and predicting prognosis in patients with non-small-cell lung cancer undergoing neoadjuvant therapy and surgery. Lung (2022) 200:393–400. doi: 10.1007/s00408-022-00541-2

[17]. Yang L, Fan X, Qin W, Xu Y, Zou B, Fan B, et al. A novel deep learning prognostic system improves survival predictions for stage iii non-small cell lung cancer. Cancer Med (2022) 11:4246–55. doi: 10.1002/cam4.4782

[18]. Kingma DP, Ba J. Adam: A method for stochastic optimization. arXiv preprint arXiv (2014) 1412:6980. doi: 10.48550/arXiv.1412.6980

[19]. Sundararajan M, Taly A, Yan Q. (2017). Axiomatic attribution for deep networks, in: Proceedings of the 34th International Conference on Machine Learning, 70 ICML'17:3319–28. doi: 10.5555/3305890.3306024

[20]. Katzman JL, Shaham U, Cloninger A, Bates J, Jiang T, Kluger Y. Deepsurv: personalized treatment recommender system using a cox proportional hazards deep neural network. BMC Med Res Method (2018) 18:1–12. doi: 10.1186/s12874-018-0482-1

[21]. Adeoye J, Koohi-Moghadam M, Lo AWI, Tsang RKY, Chow VLY, Zheng LW, et al. Deep learning predicts the malignant-transformation-free survival of oral potentially malignant disorders. Cancers (2021) 13:6054. doi: 10.3390/cancers13236054

[22]. Huang C, Dai Y, Chen Q, Chen H, Lin Y, Wu J, et al. Development and validation of a deep learning model to predict survival of patients with esophageal cancer. Front Oncol (2022) 12. doi: 10.3389/fonc.2022.971190

[23]. Lin J, Yin M, Liu L, Gao J, Yu C, Liu X, et al. The development of a prediction model based on random survival forest for the postoperative prognosis of pancreatic cancer: A seer-based study. Cancers (2022) 14:4667. doi: 10.3390/cancers14194667

[24]. Schaake-Koning C, Van den Bogaert W, Dalesio O, Festen J, Hoogenhout J, van Houtte P, et al. Effects of concomitant cisplatin and radiotherapy on inoperable non small-cell lung cancer. New Engl J Med (1992) 326:524–30. doi: 10.1056/ NEJM199202203260805

[25]. Dillman RO, Seagren SL, Propert KJ, Guerra J, Eaton WL, Perry MC, et al. A randomized trial of induction chemotherapy plus high-dose radiation versus radiation alone in stage iii non-small-cell lung cancer. New Engl J Med (1990) 323:940–5. doi: 10.1056/NEJM199010043231403

[26]. Dillman RO, Herndon J, Seagren SL, Eaton WLJr., Green MR. Improved survival in stage iii non-small-cell lung cancer: seven-year follow-up of cancer and leukemia group b (calgb) 8433 trial. JNCI. J Natl Cancer Institute (1996) 88:1210–5. doi: 10.1093/jnci/88.17.1210

[27]. Mulder R, Singh AB, Hamilton A, Das P, Outhred T, Morris G, et al. The limitations of using randomised controlled trials as a basis for developing treatment guidelines. Evidence-Based Ment Health (2018) 21:4–6. doi: 10.1136/eb-2017-102701

[28]. Pearl J. Theoretical impediments to machine learning with seven sparks from the causal revolution. arXiv preprint arXiv (2018) 1801:04016. doi: 10.1145/ 3159652.3176182

[29]. Heinze-Deml C, Meinshausen N. Conditional variance penalties and domain shift robustness. arXiv preprint arXiv (2017) 1710:11469. doi: 10.48550/ arXiv.1710.11469

[30]. Athey SC, Bryan KA, Gans JS. (2020). The allocation of decision authority to human and artificial intelligence, in: AEA Papers and Proceedings, American Economic Association 2014 Broadway, Suite 305, Nashville, TN 37203, Vol. 110. pp. 80–4. Available at: https://papers.ssrn.com/sol3/papers.cfm?abstract_id=3517287.

[31]. Cui P,Athey S. Stable learning establishes some common ground between causal inference and machine learning. Nat Mach Intell (2022) 4:110–5. doi: 10.1038/s42256 022-00445-z

[32]. Xu R, Cui P, Shen Z, Zhang X, Zhang T. Why stable learning works? a theory of covariate shift generalization. arXiv preprint arXiv:2111.02355 (2021) 2. doi: 10.48550/ arXiv.2111.02355

[33]. Kuang K, Cui P, Athey S, Xiong R, Li B. (2018). Stable prediction across unknown environments, in: Proceedings of the 24th ACM SIGKDD international conference on knowledge discovery & data mining, .pp. 1617–26. doi: 10.1145/ 3219819.3220082

[34]. Shen Z, Liu J, He Y, Zhang X, Xu R, Yu H, et al. Towards out-of-distribution generalization: A survey. arXiv preprint arXiv:2108.13624 (2021). doi: 10.48550/ arXiv.2108.13624